The 2009 IEEE/RSJ International Conference on
Intelligent Robots and Systems
October 11-15, 2009 St. Louis, USA

# Robotic Wheelchair Based on Observations of People Using Integrated Sensors

Yoshinori Kobayashi, Yuki Kinpara, Tomoo Shibusawa and Yoshinori Kuno

*Abstract*— **Recently, several robotic/intelligent wheelchairs have been proposed that employ user-friendly interfaces or autonomous functions. Although it is often desirable for user to operate wheelchairs on their own, they are often accompanied by a caregiver or companion. In designing wheelchairs, it is important to reduce the caregiver load. In this paper we propose a robotic wheelchair that can move with a caregiver side by side. In contrast to a front-behind position, in a side-by-side position it is more difficult for wheelchairs to adjust when the caregiver makes a turn. To cope with this problem we present a visual-laser tracking technique. In this technique, a laser range sensor and an omni-directional camera are integrated to observe the caregiver. A Rao-Blackwellized particle filter framework is employed to track the caregiver's position and orientation of both body and head based on the distance data and panorama images captured from the laser range sensor and the omni-directional camera. After presenting this technique, we introduce an application of the wheelchair for museum visit use.**

## I. INTRODUCTION

Over the last decade, a variety of robotic/intelligent wheelchairs have been proposed to meet the needs of an aging society. The main topics of research are user-friendly interfaces or autonomous functions such as moving toward some goal while avoiding obstacles [1], [8], [9], [10], [12].

Although it is often desirable for users to operate wheelchairs on their own, they are often accompanied by caregivers or companions. Thus, in designing wheelchair technology it is important to consider how to reduce the caregiver load and support communication between user and caregiver [5].

In this paper we propose a robotic wheelchair that moves autonomously to collaborate with a caregiver based on visual and laser sensing techniques. Moving autonomously with the caregiver does not mean simply following the caregiver. To support communication between caregiver and user, the wheelchair moves with the caregiver side by side. To reduce caregiver load, the wheelchair can see what the caregiver is doing and respond appropriately. For example, when the caregiver moves forward to push a button to call an elevator or open a door, the wheelchair waits until the elevator comes or the door is opened. Such actions can be done without any caregiver commands.

This work was supported in part by the Ministry of Education, Culture, Sports, Science and Technology under the Grant-in-Aid for Scientific Research (KAKENHI 18650043).

Y. Kobayashi, Y. Kinpara, T. Shibusawa and Y. Kuno are with the Department of Information and Computer Sciences, Saitama University, Saitama city, Saitama 338-8570, Japan {yosinori, kinpara, shibusawa, kuno}@cv.ics.saitama-u.ac.jp

To confirm the advantage of side-by-side movement we conducted a questionnaire. We showed 103 participants two types of videos. In the first, the caregiver follows the wheelchair from behind, whereas in the second, the caregiver and wheelchair move side by side (Fig.1(b)). After they watched the videos, we gave participants a list of adjectives (in Japanese) and asked them to assign a value from 1 to 6 (6: definitely yes to 1: definitely no) that conveys their feeling about the relationship between the caregiver and user. Results are shown in Fig.1(a). Scores for moving side by side are significantly higher than those for following behind in all question cases ($p < 0.05$). For the direct question, "Which wheelchair do you prefer?" 86 out of 103 participants selected the side-by-side case. These results suggest an advantage to our proposal.

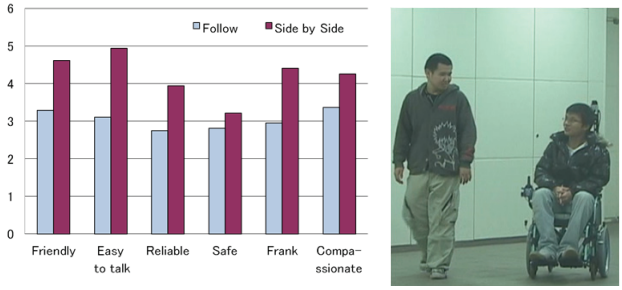


(a) Result of questionnaire (b) Sample of video images

Fig. 1. Wheelchair moving with caregiver side by side

To develop a system that can support side-by-side movement, we propose a novel visual-laser tracking technique. A laser range sensor and an omni-directional camera are integrated to track the caregiver's position and motion. Both devices are installed on top of the pole placed on the seat back.

While several methods for tracking people using laser range sensor have been proposed, most of these use fixed laser range sensors placed near the floor, and track positions of people by observing their legs [2]. Glas et al. [4] proposed a particle filter based method that can track human body motion using adaptive shape modeling. However they assume observations from multiple fixed laser range sensors distributed in the environment.

In contrast, we employ the Rao-Blackwellized particle filter framework [11], [14] to track caregiver position and orientation of both the body and the head based on the distance data and panorama images captured from the laser range sensor and omni-directional camera, respectively. Distance

data is mapped onto a 2D image plane and used for the likelihood evaluation in the Rao-Blackwellized particle filter framework. The likelihoods of the hypotheses are evaluated from the contour similarity between the model and the caregiver's upper body that is partially observed by a single laser range sensor.

Cui et al. [3] reported a method to track people by using laser range sensors and cameras. In their method, multiple cameras are employed to identify the person being tracked. Our approach is to integrate vision and laser based observations for precise tracking of behavior. Our method can track, for example, face direction by integrating panorama images from the omni-directional camera and distance data from the laser range sensor.

We also present an application of our robotic wheelchair dedicated to museum visit use. With the visual-laser tracking technique, the wheelchair user and caregiver move together side by side. When the caregiver stops close to an exhibit, the wheelchair detects the exhibit with its other vision system and moves to the position where the user can view the exhibit. For this purpose our wheelchair is equipped with a pan-tilt camera that moves synchronously with the caregiver's head motion. In addition, the wheelchair turns towards the caregiver when the caregiver turns toward the user to talk about the exhibit. In this way, our wheelchair responds depending on the situation.

The remainder of this paper is organized as follows. In the next section, we describe our tracking method using integrated sensors. In section 3, we describe the method for controlling the wheelchair. In section 4, we explain our experiments and discuss about the experimental results. In section 5, we propose an application of our robotic wheelchair for museum visit. Finally, we summarize our work.

## II. Tracking Caregiver

In this section we describe the method for tracking caregiver position and motion. First, we introduce our integrated device.

### A. Device integration

Fig.2 shows an overview of our visual-laser tracker. An omni-directional camera (WAT-240 by Watec) is installed on top of a laser range sensor (URG-04LX by Hokuyo Electric Machinery). This sensor can measure 270 degrees and 20mm〜4000mm in distance. The omni-directional camera observes target appearances and the laser range sensor measures target distance. Each device has a fully overlapping field of sensing. As a result, our sensor setup is effective and complementary.

In the following section we describe details of our tracking method based on the Rao-Blackwellized particle filter framework.

### B. Modeling caregiver as tracking target

The caregiver is modeled as shown in Fig.3(a). We assume that the laser range sensor is placed horizontally on the caregiver's shoulder level so that the contour of the

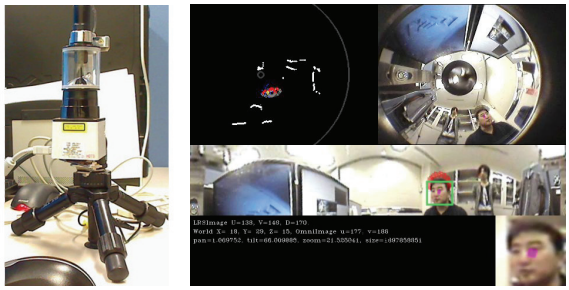

(a) Device (b) Example of display image

Fig. 2. Visual-laser tracker

caregiver's shoulder can be observed. When the distance data captured with the laser range sensor is mapped onto the 2D image plane (what we call a "laser image"), the contour of the caregiver's shoulder is partially observed as shown in Fig.3(b). The contour of the caregiver's shoulder can be observed as a part of an ellipse. We use the ellipse as the model to track the position and the direction of the caregiver's body. In Fig.3(b), points on the contour indicate evaluation points, which are used in the likelihood evaluation step. The caregiver's head position and direction are also tracked using an omni-directional camera. We use an ellipsoid as a model to track the caregiver's head.

We assume the coordinate system represented by their $X$- and $Y$-axes aligned on the ground plane, and the $Z$-axis representing the vertical direction from the ground plane. We assume that the caregiver walks alongside with the wheelchair without tilting his or her head. The model of the tracking target is represented with center coordinates of the ellipse $[u, v]$, rotation of the ellipse $\phi$, center coordinates of the ellipsoid $[x, y, z]$ and rotation of the ellipsoid around the $Z$-axis $\theta$. State variables of the tracking target are denoted by $\{u, v, \phi, x, y, z, \theta\}$. Note that $\theta$ can take the value from $\phi - 90$ to $\phi + 90$, because humans do not typically turn their head more than 90 degrees.

In the next section we describe the method of tracking using the Rao-Blackwellized particle filter.

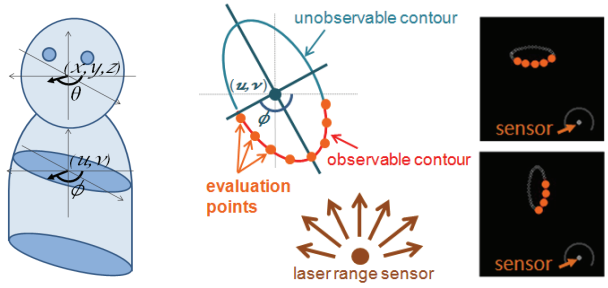


(a) Human model (b) Body contour model

Fig. 3. Human body model

### C. Rao-Blackwellized particle filter

Denotes the state to be estimated as $X$, and observation $Z$, with subscript time index $t$. The key idea of the Rao-Blackwellized particle filter (RBPF) is to partition the original state space $X_t$ into two sub-state spaces $R_t$ (root vari-

ables) and $L_t$ (leaf variables). Factorization of the probability is denoted by

$$p(X_{1:t}|Z_{1:t}) = p(L_{1:t}, R_{1:t}|Z_{1:t}) = p(L_{1:t}|R_{1:t}, Z_{1:t})p(R_{1:t}|Z_{1:t}). \quad (1)$$

If we assume that $p(L_{1:t}|R_{1:t}, Z_{1:t})$ can be computed through a linear process, a non-linear non-Gaussian state space is much smaller than $p(X_{1:t}|Z_{1:t})$. Thus the RBPF will provide better performance than the regular particle filter [6] while using the same number of particles. For this advantage, the RBPF is known to be effective in tracking objects with complex structures. Xu et al. [14] details the application of RBPF in the field of visual surveillance.

When we assume that caregivers do not bend their body while walking with the wheelchair, we can consider a strong relationship between the center of the body and the center of head. If the laser range sensor and omni-directional camera are strongly calibrated with respect to each other, the object that is observed with the laser range sensor is easily projected onto the omni-directional camera image. Then, when the center location of the body contour ellipse and the height of the caregiver's head are given, we can roughly estimate the location of the caregiver's head in the omni-directional camera image. Based on this we can partition original state space into two groups: root variables, $R_t = \{u_t, v_t, \phi_t, \theta_t\}$ and leaf variables $L_t = \{x_t, y_t, z_t\}$.

We assume a relationship between components as shown in Fig.4. The caregiver's body position and orientation and head orientation at time $t$ ($R_t$) only depends on the previous state $R_{t-1}$, while the center of the head position at time $t$ ($L_t$) depends on the previous state $L_{t-1}$ and current root state $R_t$. The observations at time $t$ ($Z_t$) depend on both current states $R_t$ and $L_t$.

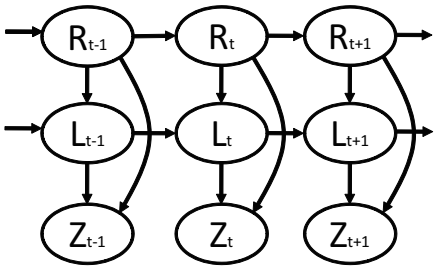


Fig. 4. Dependency relationship between components for the RBPF

As regular particle filters, RBPFs represent posterior distribution using a set of weighted samples $S_t = \{s_t^{(i)}, w_t^{(i)} \mid 1 \leq i \leq N\}$. $R^{(i)}$ in each particle $s^{(i)}$ is sampled from $p(R_{1:t}|Z_{1:t})$ in a similar way as in the regular particle filter. $L^{(i)}$ in each particle $s^{(i)}$ is generated by computing the linear process corresponding to $p(L_{1:t}|R_{1:t}, Z_{1:t})$.

Based on the dependency model (Fig.4), $\hat{R}_t^{(i)}$ in each particle $\hat{s}_t^{(i)}$ is sampled from:

$$\hat{R}_t^{(i)} \sim p(R_t|R_{t-1}^{(i)}, Z_t). \quad (2)$$

This means that a hypothesis on a new body location and orientation and head orientation will be propagated by the motion model. Here we employ a simple random walk model as the motion model $\hat{R}_t^{(i)} = R_{t-1}^{(i)} + N_r$, where $N_r$ is a random vector drawn from the system noise. Though we may consider another motion model such as uniform motion, in this case the system performs robust and stable tracking even when we employ the simplest motion model.

The $\hat{L}_t^{(i)}$ is computed using:

$$\hat{L}_t^{(i)} \sim p(L_t|R_t^{(i)}, L_{t-1}^{(i)}, Z_t). \quad (3)$$

This means that a new head location hypothesis $\hat{L}_t^{(i)}$ will be generated based on the previous location of the head $L_{t-1}^{(i)}$ and current state $\hat{R}_t^{(i)}$.

Here we employ the model in which the head location on the $XY$ plane $\hat{x}_t^{(i)}, \hat{y}_t^{(i)}$ is estimated by using Kalman filtering based on the values $\hat{u}_{t-1}^{(i)}, \hat{v}_{t-1}^{(i)}$ in $\hat{R}_{t-1}^{(i)}$ and $\hat{u}_t^{(i)}, \hat{v}_t^{(i)}$ in $\hat{R}_t^{(i)}$. The head location along the $Z$-axis $\hat{z}_t^{(i)}$ is the same as the value of $z_{t-1}^{(i)}$ in $L_{t-1}^{(i)}$ with Gaussian noise $N_l$.

Now that all of the state variables in each particle $\hat{s}_t^{(i)}$ can be obtained, we can evaluate each particle the same as a regular particle filter.

### D. Likelihood evaluation

Here we evaluate particles based on the observations of the laser range sensor and the omni-directional camera, and then integrate the results of the evaluations.

**Likelihood evaluation based on laser image**

The likelihood is evaluated by the maximum distance between evaluation points and the nearest distance data using:

$$w_{t,laser}^{(i)} = \exp\left(\frac{-d_{max}^2}{\sigma_d}\right). \quad (4)$$

Where $w_{t,laser}^{(i)}$ is the likelihood score based on the laser image. The $d_{max}$ is the maximum distance between evaluation points and the nearest distance data. At each time instance, once the distance image is generated from the laser image, each distance $d_n$ is easily obtained. The $\sigma_d$ is the variance derived from $d_n$.

Conceptional images of evaluation process are shown in Fig.5. The likelihood of each particle is evaluated as in Fig.5(a). The likelihood score is maximized when the model completely matches the laser image and we can also guess the head position on the $XY$ plane (Fig.5(b)).

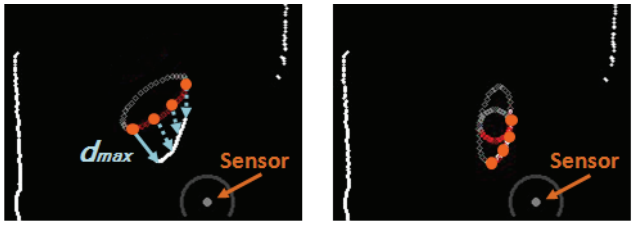


(a) Evaluation based on maximum distance (b) Completely matching case

Fig. 5. Likelihood evaluation

**Likelihood evaluation based on omni-directional camera image**

We use the state variables $\hat{x}_t^{(i)}, \hat{y}_t^{(i)}, \hat{z}_t^{(i)}$ and $\hat{\theta}_t^{(i)}$ in particle $\hat{s}_t^{(i)}$ for evaluating a particle using the AdaBoost-based cascaded classifiers [13]. Since our integrated device is fully calibrated, we can project these variables onto the calibrated omni-directional camera image. We evaluate particles by applying the AdaBoost-based cascaded classifiers over the projected image region and the number of stages passed in the cascade is employed as the likelihood of a human head. While an abstracted evaluation procedure is given below, the detailed evaluation method is provided in [7].

Note that we use 7 classifiers and each classifier is trained respectively to detect a human head of a particular direction such as front, 90° left, 90° right and so on.

1) Project the state variables $\hat{x}_t^{(i)}, \hat{y}_t^{(i)}, \hat{z}_t^{(i)}$ and $\hat{\theta}_t^{(i)}$ onto the calibrated omni-directional camera image and obtain a projected position and size of the head. By considering the location and the direction of a head, we can also calculate the direction of a human head relative to the omni-directional camera $\hat{\theta}_{t,cam}^{(i)}$.
2) Extract an image region corresponding to the head and extend it into a normal image based on its position and size.
3) Resize the extracted image region to input the classifier (e.g.24×24 pixel). We then obtain the classifier input image $g_t^{(i)}$.
4) Select a classifier by considering the direction of a human head relative to the omni-directional camera $\hat{\theta}_{t,cam}^{(i)}$. For example, if we use three classifiers such as front, 90° left and 90° right, then the front is selected in the case of $-45° \leq \theta_{t,cam}^{(i)} \leq 45°$, the 90° left is selected in the case of $45° < \theta_{t,cam}^{(i)} \leq 135°$ and so on.
5) Apply the selected classifier to the image region $g_t^{(i)}$ and obtain the likelihood score of a human head $w_{t,cam}^{(i)}$.

**Likelihood integration**

To obtain the weight $w_t^{(i)}$ for the particle $s_t^{(i)}$ the weights $w_{t,laser}^{(i)}$ and $w_{t,cam}^{(i)}$ are consolidated using:

$$w_t^{(i)} = w_{t,laser}^{(i)} \cdot w_{t,cam}^{(i)}. \quad (5)$$

These likelihood evaluation procedures are repeated for each particle. The estimation of the state at time $t$ is calculated as the expectation of the weights over particles.

## III. Controlling the Wheelchair

### A. System overview

Fig.6 shows an overview of our robotic wheelchair. For the autonomous function, we attach the visual-laser tracker on the rear pole as shown in Fig.6. This integrated device is used to track the caregiver. A pan-tilt camera is also attached on top of the rear pole to detect an object. The wheelchair has another range sensor (UTM-30LX by Hokuyo Electric Machinery) facing forward to detect pedestrians and obstacles.

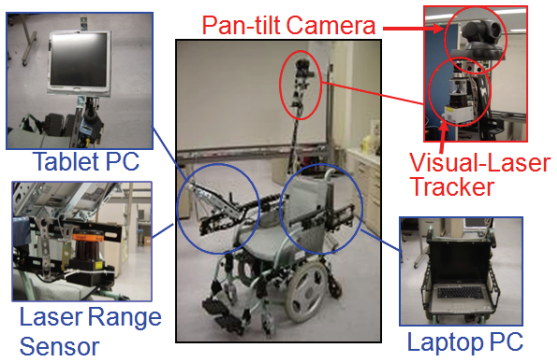


Fig. 6. Overview of our robotic wheelchair

### B. Controlling wheelchair from PC

Our wheelchair can be controlled with a joystick controller. We attach an extension unit to the joystick for controlling the output signal. This unit is connected to a laptop PC with serial connection and is controlled by our software. The relation of the joystick position and output signal is shown in Table I. This output signal is controlled using two output voltage values that are a front-back control voltage and a left-right control voltage. These voltage values are controlled using the extension unit that includes a D/A converter.

TABLE I
VOLTAGE AND CONTROL SIGNAL

| Voltage | 0-1.7[v] | 1.7-2.9[v] | 2.9-5[v] |
|---|---|---|---|
| Front-Back Control | Backward | Neutral | Forward |
| Left-Right Control | Right-side | Neutral | Left-side |

### C. Following the caregiver

Our robotic wheelchair usually moves with the caregiver side by side. The speed and direction of the robotic wheelchair are controlled using the information of the caregiver (Fig.7). We take the $X$ axis in the left-right direction of the wheelchair and the $Y$ axis in the front-back direction. The initial position ($u_0$,$v_0$) of the caregiver is assumed to be the standard location of the caregiver (Fig.7(a)). The speed is controlled based on the difference ($\Delta u$,$\Delta v$) of the current caregiver's position from the initial position. If the difference is positive, the speed is increased, whereas if it is negative, the speed is decreased. When the current position is not different from the previous position, the system considers that the caregiver is moving at the same speed and the robotic wheelchair is following him or her at the same speed.

The moving direction is controlled based on the caregiver's position and body direction. When the caregiver turns his or her body near the wheelchair the wheelchair also turns in the same direction. If the caregiver turns towards the wheelchair, the wheelchair slows down and waits a bit for the caregiver because the wheelchair will be in the caregiver's path if it does not slow down.

## IV. Experimental Results

We set up our visual-laser tracker on the top of the camera mount (130cm high) to confirm the tracking performance. A

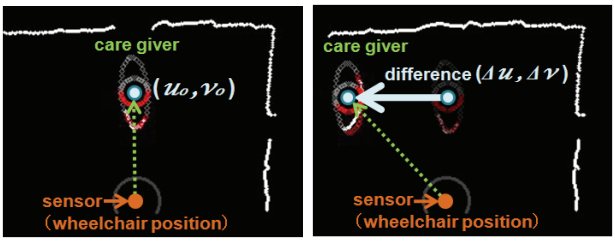


(a) Initial position (b) Difference cue

Fig. 7. Wheelchair moving by difference cue

person walking on the previously determined trajectory is tracked using our tracker. We assign the parameter $\sigma_d$ the value 5 for computational convenience. As shown in Fig.8(a), our tracker successfully tracks the person who is walking while changing body direction. The average Euclidean distance between the tracked position and the ground truth for the $XY$ plane is 5.8 cm.

We also confirm the tracking performance of the body and head direction. The person rotating in front of our tracker is recorded by the video camera mounted on the ceiling looking downward. Tracking errors are shown in Fig.8(b) where the error value is obtained by comparing the tracking result and the manually extracted direction. The average error of the body direction is 5.2 degrees and head direction is 23.4 degree. The body direction of the person is precisely tracked. The head direction is also precisely tracked considering the low resolution of images captured with the omni-directional camera.

We conducted an experiment on our robotic wheelchair that follows the caregiver side by side. Fig.9 shows trajectories of the caregiver and wheelchair. The wheelchair successfully follows the caregiver even when the caregiver turns towards the left or right. It is difficult to turn towards the left when the wheelchair moves along the left side of the caregiver because the caregiver cannot move towards the left due to the wheelchair being in caregiver's path. We can deal with this situation by considering the caregiver's body direction.

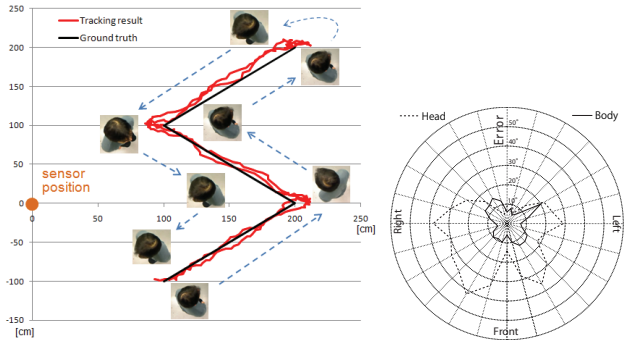


(a) Trajectory errors (b) Direction errors

Fig. 8. Tracking Performance

## V. Application for Art Appreciation

In this application the wheelchair user and caregiver normally move together side by side. When the caregiver finds an exhibit and stops close to it, the wheelchair detects this and moves to a position where the wheelchair user can view the exhibit.

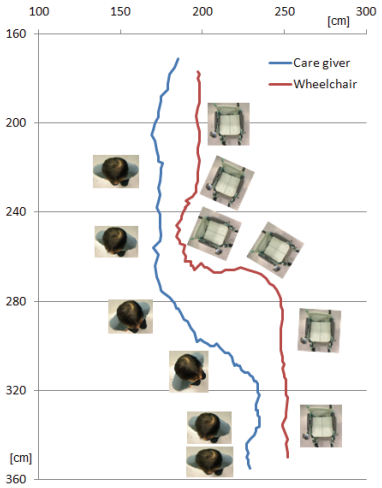


Fig. 9. Trajectories of caregiver and wheelchair

### A. Detecting a painting

Since we propose an application for supporting art appreciation in a typical scenario, here we assume that the exhibit is a painting so that can be detected using template matching. We have prepared four template-images to detect four corners of the target painting in advance. The system searches for the four template-image locations in the image captured with the pan-tilt camera. After the locations are detected, the system detects the painting by considering the consistency of arrangement of the four corners. The ratio of right and left edges of the painting is used to estimate the relative position of the wheelchair with respect to the painting.

### B. Moving to viewing position

Fig.10 and Fig.11 show an example of a sequence of actions to support viewing an exhibit. Figs.11 (a)-(d) show images at points (a)-(d) in Fig.10, respectively.

When the wheelchair detects that the caregiver has stopped walking, the visual-laser tracker detects the face direction of the caregiver. The system then tries to detect the object that the caregiver is looking at using the pan-tilt camera that is synchronized with the caregiver's head direction. The direction in where the caregiver is looking can be used to restrict the search region to detect an exhibit (Figs.10,11(a)). Then, the wheelchair starts moving to a position where the user can view the painting (Figs.10,11(b)-(c)). The wheelchair controls its motion using visual feedback. It adjusts its position until the four corners of the painting come to the center of the image captured with the pan-tilt camera at the original pan-tilt position (Figs.10,11(d)).

When the caregiver turns towards the wheelchair user to talk about the painting, the wheelchair turns towards the caregiver. When the caregiver turns towards the painting again, the wheelchair makes the same action.

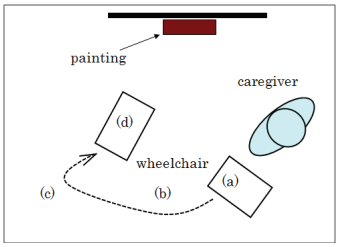


Fig. 10. Wheelchair movements in painting appreciation

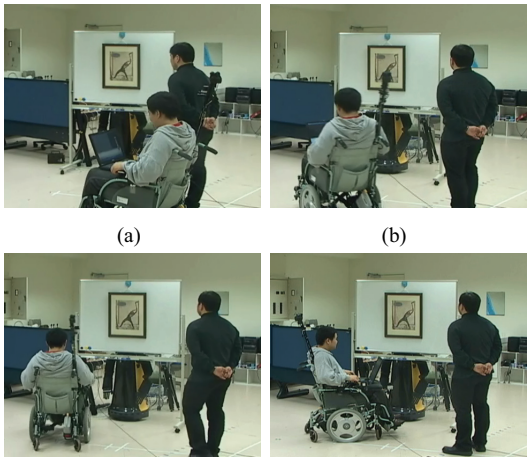

(a) (b) (c) (d)

Fig. 11. Example of supporting art appreciation

## VI. CONCLUSIONS AND FUTURE WORKS

In this paper, we have proposed a visual-laser tracking technique applied to a collaborative robotic wheelchair. A laser range sensor and an omni-directional camera are integrated to observe the caregiver's behavior. The RBPF framework is employed to track the caregiver's position and orientation of the body and head. The likelihood of particles is evaluated based on the distance data from the laser range sensor and panorama images from the omni-directional camera. In addition, we proposed a robotic wheelchair system based on the proposed tracking techniques. The wheelchair follows the caregiver side by side. When the caregiver turns his or her body towards the wheelchair, the wheelchair slows down and waits for the caregiver in order to avoid obstructing the caregiver's path. The wheelchair successfully follows the caregiver even when the caregiver turns towards the left or right. We have also proposed an application of our robotic wheelchair for supporting the viewing of exhibits in museums. In particular, when the caregiver stops in front of an exhibit, the wheelchair moves autonomously to a position suitable for viewing the exhibit.

In future work, we are planning to give our wheelchair functions for avoiding moving obstacles such as pedestrians. We have begun to deal with this problem by tracking pedestrians based on the Kalman filter and have started to conduct trials (Fig.12). We also consider developing recovering functions. When the wheelchair has lost track of the caregiver, the system tries to detect the caregiver based on appearance and spatio-temporal cues. In other future work we would like to establish a method to identify the caregiver among people around the wheelchair, because the system needs to track the caregiver continuously even when he or she is temporary occluded by obstacles.

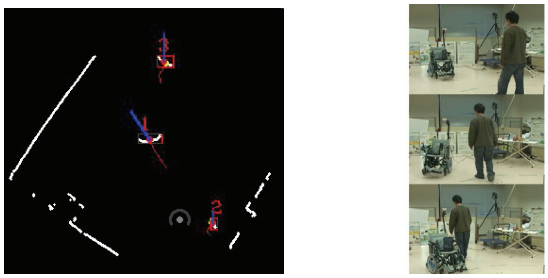

(a) Pedestrian tracking (b) Avoiding pedestrian

Fig. 12. Wheelchair avoiding obstacles

## VII. ACKNOWLEDGMENTS

The authors gratefully acknowledge the members of Advanced Technology R&D Center, Mitsubishi Electric Corporation, for their contribution to provide their expertise.

## REFERENCES

[1] E.S. Boy, C.L. Teo and E. Burdet, "Collaborative Wheelchair Assistant," *Proc. IEEE/RSJ International Conference on Intelligent Robots and Systems*, vol.2, pp.1511-1516, 2002.

[2] J. Cui, H. Zha, H. Zhao and R. Shibasaki, "Fusion of Detection and Matching Based Approaches for Laser Based Multiple People Tracking," *Proc. International Conference on Computer Vision and Pattern Recognition*, vol.1, pp.642-649, 2006.

[3] J. Cui, H. Zha, H. Zhao and R. Shibasaki, "Tracking multiple people using laser and vision," *Proc. IEEE/RSJ International Conference on Intelligent Robots and Systems*, pp.1301-1306, 2005.

[4] D.F. Glas, T. Miyashita, H. Ishiguro and N. Hagita, "Laser tracking of human body motion using adaptive shape modeling," *Proc. IEEE/RSJ International Conference on Intelligent Robots and Systems*, pp.602-608, 2007.

[5] T. Iwase, R. Zhang and Y. Kuno, "Robotic Wheelchair Moving with the Caregiver," *Proc. SICE-ICASE International Joint Conference 2006*, pp.238-243, 2006.

[6] M. Isard and A. Blake, "Condensation - Conditional Density Propagation for Visual Tracking," *International Journal of Computer Vision*, vol.29, no.1, pp.5-28, 1998.

[7] Y. Kobayashi, D. Sugimura, Y. Sato, H. Hirasawa, N. Suzuki, H. Kage and A. Sugimoto, "3D Head Tracking using the Particle Filter with Cascaded Classifiers," *Proc. British Machine Vision Conference*, pp.37-46, 2006.

[8] Y. Kuno, N. Shimada and Y. Shirai, "Look Where You're Going: A Robotic Wheelchair Based on the Integration of Human and Environmental Observations," *IEEE Robotics and Automation*, vol.10, no.1, pp.26-34, 2003.

[9] S.P. Levine, D.A. Bell, L.A. Jaros, R.C. Simpson, Y. Koren, and J. Borenstein, "The NavChair Assistive Wheelchair Navigation System," *IEEE Trans. Rehabilitation Engineering*, vol.7, pp.443-451, 1999.

[10] J. Min, K. Lee, S. Lim and D. Kwon, "Human-Friendly Interfaces of Wheelchair Robotic System for Handicapped Persons," *Proc. IEEE/RSJ International Conference on Intelligent Robots and Systems*, vol.2, pp.1505-1510, 2002.

[11] K. Murphy and S. Russell, "Rao-Blackwellised Particle Filtering for Dynamic Bayesian Networks," *Sequential Monte Carlo Methods in Practice*, Springer-Verlag, pp.500-512, 2001.

[12] Y. Satoh and K. Sakaue, "An Omnidirectional Stereo Vision-Based Smart Wheelchair," *Journal on Image and Video Processing*, vol.2007, 87646, 2007.

[13] P. Viola and M. Jones, "Rapid Object Detection Using a Boosted Cascade of Simple Features," *Proc. IEEE International Conference on Computer Vision and Pattern Recognition*, vol.1, pp.511-518, 2001.

[14] X. Xu and B. Li, "Rao-Blackwellised Particle Filter for Tracking with Application in Visual Surveillance," *Proc. International Conference on Computer Communications and Networks*, pp.17-24, 2005.